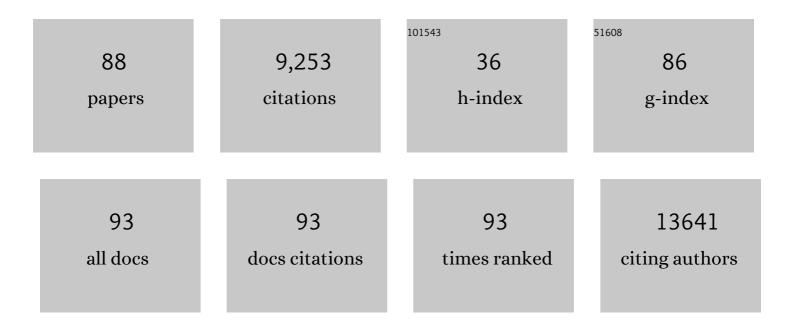
List of Publications by Year in descending order

Source: https://exaly.com/author-pdf/206727/publications.pdf Version: 2024-02-01



KEITH T RUTLED

| # | Article | IF | CITATIONS |
|----|--|------|-----------|
| 1 | Machine learning for molecular and materials science. Nature, 2018, 559, 547-555. | 27.8 | 2,387 |
| 2 | Atomistic Origins of High-Performance in Hybrid Halide Perovskite Solar Cells. Nano Letters, 2014, 14, 2584-2590. | 9.1 | 2,068 |
| 3 | Molecular ferroelectric contributions to anomalous hysteresis in hybrid perovskite solar cells. APL Materials, 2014, 2, . | 5.1 | 481 |
| 4 | Ferroelectric materials for solar energy conversion: photoferroics revisited. Energy and Environmental Science, 2015, 8, 838-848. | 30.8 | 333 |
| 5 | Heterogeneous catalytic hydrogenation of CO ₂ by metal oxides: defect engineering – perfecting imperfection. Chemical Society Reviews, 2017, 46, 4631-4644. | 38.1 | 304 |
| 6 | Interplay of Orbital and Relativistic Effects in Bismuth Oxyhalides: BiOF, BiOCl, BiOBr, and BiOI. Chemistry of Materials, 2016, 28, 1980-1984. | 6.7 | 291 |
| 7 | Electronic Chemical Potentials of Porous Metal–Organic Frameworks. Journal of the American Chemical Society, 2014, 136, 2703-2706. | 13.7 | 262 |
| 8 | Best practices in machine learning for chemistry. Nature Chemistry, 2021, 13, 505-508. | 13.6 | 240 |
| 9 | Band alignment of the hybrid halide perovskites CH ₃ NH ₃ PbCl ₃ , CH ₃ NH ₃ PbBr ₃ and CH ₃ NH ₃ Pbl ₃ . Materials Horizons, 2015, 2, 228-231. | 12.2 | 238 |
| 10 | How Strong Is the Hydrogen Bond in Hybrid Perovskites?. Journal of Physical Chemistry Letters, 2017, 8, 6154-6159. | 4.6 | 174 |
| 11 | Relativistic electronic structure and band alignment of BiSI and BiSel: candidate photovoltaic materials. Journal of Materials Chemistry A, 2016, 4, 2060-2068. | 10.3 | 127 |
| 12 | Computational Screening of All Stoichiometric Inorganic Materials. CheM, 2016, 1, 617-627. | 11.7 | 115 |
| 13 | Polymorph Engineering of TiO ₂ : Demonstrating How Absolute Reference Potentials Are Determined by Local Coordination. Chemistry of Materials, 2015, 27, 3844-3851. | 6.7 | 113 |
| 14 | Prediction of Electron Energies in Metal Oxides. Accounts of Chemical Research, 2014, 47, 364-372. | 15.6 | 107 |
| 15 | Computational materials design of crystalline solids. Chemical Society Reviews, 2016, 45, 6138-6146. | 38.1 | 105 |
| 16 | Band Engineering of Carbon Nitride Monolayers by N-Type, P-Type, and Isoelectronic Doping for Photocatalytic Applications. ACS Applied Materials & Interfaces, 2018, 10, 11143-11151. | 8.0 | 92 |
| 17 | Electronic Structure Modulation of Metal–Organic Frameworks for Hybrid Devices. ACS Applied Materials & Interfaces, 2014, 6, 22044-22050. | 8.0 | 75 |
| 18 | Designing interfaces in energy materials applications with first-principles calculations. Npj Computational Materials, 2019, 5, . | 8.7 | 71 |

| # | Article | IF | CITATIONS |
|----|--|------|-----------|
| 19 | Role of entropic effects in controlling the polymorphism in formate ABX ₃ metal–organic frameworks. Chemical Communications, 2015, 51, 15538-15541. | 4.1 | 66 |
| 20 | Organised chaos: entropy in hybrid inorganic–organic systems and other materials. Chemical Science, 2016, 7, 6316-6324. | 7.4 | 62 |
| 21 | Interpretable and Explainable Machine Learning for Materials Science and Chemistry. Accounts of Materials Research, 2022, 3, 597-607. | 11.7 | 60 |
| 22 | Quasi-particle electronic band structure and alignment of the V-VI-VII semiconductors SbSI, SbSBr, and SbSeI for solar cells. Applied Physics Letters, 2016, 108, . | 3.3 | 59 |
| 23 | Tuning the Negative Thermal Expansion Behavior of the Metal–Organic Framework Cu ₃ BTC ₂ by Retrofitting. Journal of the American Chemical Society, 2019, 141, 10504-10509. | 13.7 | 57 |
| 24 | Role of Amine–Cavity Interactions in Determining the Structure and Mechanical Properties of the Ferroelectric Hybrid Perovskite [NH ₃ NH ₂]Zn(HCOO) ₃ . Chemistry of Materials, 2016, 28, 312-317. | 6.7 | 55 |
| 25 | Computer-aided design of metal chalcohalide semiconductors: from chemical composition to crystal structure. Chemical Science, 2018, 9, 1022-1030. | 7.4 | 54 |
| 26 | Crystal electron binding energy and surface work function control of tin dioxide. Physical Review B, 2014, 89, . | 3.2 | 48 |
| 27 | Microscopic origin of entropy-driven polymorphism in hybrid organic-inorganic perovskite materials. Physical Review B, 2016, 94, . | 3.2 | 48 |
| 28 | Assessment of Hybrid Organic–Inorganic Antimony Sulfides for Earth-Abundant Photovoltaic Applications. Journal of Physical Chemistry Letters, 2015, 6, 5009-5014. | 4.6 | 47 |
| 29 | Origin of Ferroelectricity in Two Prototypical Hybrid Organic–Inorganic Perovskites. Journal of the American Chemical Society, 2022, 144, 816-823. | 13.7 | 47 |
| 30 | An Unusual Phase Transition Driven by Vibrational Entropy Changes in a Hybrid Organic–Inorganic Perovskite. Angewandte Chemie - International Edition, 2018, 57, 8932-8936. | 13.8 | 46 |
| 31 | Metal-free perovskites for non linear optical materials. Chemical Science, 2019, 10, 8187-8194. | 7.4 | 46 |
| 32 | Screening procedure for structurally and electronically matched contact layers for high-performance solar cells: hybrid perovskites. Journal of Materials Chemistry C, 2016, 4, 1149-1158. | 5.5 | 45 |
| 33 | Data-Driven Discovery of Photoactive Quaternary Oxides Using First-Principles Machine Learning. Chemistry of Materials, 2019, 31, 7221-7230. | 6.7 | 45 |
| 34 | Machine learning and big scientific data. Philosophical Transactions Series A, Mathematical, Physical, and Engineering Sciences, 2020, 378, 20190054. | 3.4 | 43 |
| 35 | Chemical principles for electroactive metal–organic frameworks. MRS Bulletin, 2016, 41, 870-876. | 3.5 | 42 |
| 36 | Electronic structure design for nanoporous, electrically conductive zeolitic imidazolate frameworks. Journal of Materials Chemistry C, 2017, 5, 7726-7731. | 5.5 | 40 |

| # | Article | IF | CITATIONS |
|----|--|------|-----------|
| 37 | Halide Perovskite Heteroepitaxy: Bond Formation and Carrier Confinement at the PbS–CsPbBr ₃ Interface. Journal of Physical Chemistry C, 2017, 121, 27351-27356. | 3.1 | 40 |
| 38 | Designing porous electronic thin-film devices: band offsets and heteroepitaxy. Faraday Discussions, 2017, 201, 207-219. | 3.2 | 36 |
| 39 | Lone-Pair Stabilization in Transparent Amorphous Tin Oxides: A Potential Route to p-Type Conduction Pathways. Chemistry of Materials, 2016, 28, 4706-4713. | 6.7 | 33 |
| 40 | Structural and electronic properties of silver/silicon interfaces and implications for solar cell performance. Physical Review B, 2011, 83, . | 3.2 | 32 |
| 41 | The effect of bean origin and temperature on grinding roasted coffee. Scientific Reports, 2016, 6, 24483. | 3.3 | 31 |
| 42 | A deep convolutional neural network for real-time full profile analysis of big powder diffraction data. Npj Computational Materials, 2021, 7, . | 8.7 | 31 |
| 43 | Hydrogen Bonding versus Entropy: Revealing the Underlying Thermodynamics of the Hybrid Organic–Inorganic Perovskite [CH ₃ NH ₃]PbBr ₃ . Chemistry of Materials, 2018, 30, 8782-8788. | 6.7 | 29 |
| 44 | Experimental Evidence for Vibrational Entropy as Driving Parameter of Flexibility in the Metal–Organic Framework ZIF-4(Zn). Chemistry of Materials, 2019, 31, 8366-8372. | 6.7 | 29 |
| 45 | Modeling the dielectric constants of crystals using machine learning. Journal of Chemical Physics, 2020, 153, 024503. | 3.0 | 29 |
| 46 | Band energy control of molybdenum oxide by surface hydration. Applied Physics Letters, 2015, 107, . | 3.3 | 26 |
| 47 | Realistic Surface Descriptions of Heterometallic Interfaces: The Case of TiWC Coated in Noble Metals. Journal of Physical Chemistry Letters, 2016, 7, 4475-4482. | 4.6 | 24 |
| 48 | Subwavelength Spatially Resolved Coordination Chemistry of Metal–Organic Framework Glass Blends. Journal of the American Chemical Society, 2018, 140, 17862-17866. | 13.7 | 23 |
| 49 | The chemical forces underlying octahedral tilting in halide perovskites. Journal of Materials Chemistry C, 2018, 6, 12045-12051. | 5.5 | 23 |
| 50 | Accelerated optimization of transparent, amorphous zinc-tin-oxide thin films for optoelectronic applications. APL Materials, 2019, 7, . | 5.1 | 23 |
| 51 | Materials discovery by chemical analogy: role of oxidation states in structure prediction. Faraday Discussions, 2018, 211, 553-568. | 3.2 | 22 |
| 52 | Crystal structure optimisation using an auxiliary equation of state. Journal of Chemical Physics, 2015, 143, 184101. | 3.0 | 21 |
| 53 | Understanding dynamic properties of materials using neutron spectroscopy and atomistic simulation. Journal of Physics Communications, 2020, 4, 072001. | 1.2 | 21 |
| 54 | SMACT: Semiconducting Materials by Analogy and Chemical Theory. Journal of Open Source Software, 2019, 4, 1361. | 4.6 | 21 |

| # | Article | IF | CITATIONS |
|----|---|------|-----------|
| 55 | Finding a junction partner for candidate solar cell absorbers enargite and bournonite from electronic band and lattice matching. Journal of Applied Physics, 2019, 125, . | 2.5 | 19 |
| 56 | Chemical bonding at the metal–organic framework/metal oxide interface: simulated epitaxial growth of MOF-5 on rutile TiO ₂ . Journal of Materials Chemistry A, 2017, 5, 6226-6232. | 10.3 | 18 |
| 57 | Theory of ionization potentials of nonmetallic solids. Physical Review B, 2017, 95, . | 3.2 | 18 |
| 58 | Molecular dynamics studies of the bonding properties of amorphous silicon nitride coatings on crystalline silicon. Journal of Applied Physics, 2011, 110, . | 2.5 | 14 |
| 59 | Entropy-based active learning of graph neural network surrogate models for materials properties. Journal of Chemical Physics, 2021, 155, 174116. | 3.0 | 14 |
| 60 | Quick-start guide for first-principles modelling of semiconductor interfaces. JPhys Energy, 2019, 1, 016001. | 5.3 | 12 |
| 61 | Tilt and shift polymorphism in molecular perovskites. Materials Horizons, 2021, 8, 2444-2450. | 12.2 | 12 |
| 62 | Cycling Rateâ€Induced Spatiallyâ€Resolved Heterogeneities in Commercial Cylindrical Liâ€Ion Batteries. Small Methods, 2021, 5, e2100512. | 8.6 | 12 |
| 63 | A computational investigation of nickel (silicides) as potential contact layers for silicon photovoltaic cells. Journal of Physics Condensed Matter, 2013, 25, 395003. | 1.8 | 10 |
| 64 | Morphological control of band offsets for transparent bipolar heterojunctions: The BÃ d eker diode. Physica Status Solidi (A) Applications and Materials Science, 2015, 212, 1461-1465. | 1.8 | 10 |
| 65 | Analysis of electrostatic stability and ordering in quaternary perovskite solid solutions. Physical Review B, 2016, 93, . | 3.2 | 10 |
| 66 | An Unusual Phase Transition Driven by Vibrational Entropy Changes in a Hybrid Organic–Inorganic Perovskite. Angewandte Chemie, 2018, 130, 9070-9074. | 2.0 | 10 |
| 67 | Distributed representations of atoms and materials for machine learning. Npj Computational Materials, 2022, 8, . | 8.7 | 9 |
| 68 | Electroactive Nanoporous Metal Oxides and Chalcogenides by Chemical Design. Chemistry of Materials, 2017, 29, 3663-3670. | 6.7 | 8 |
| 69 | Revealing the Potential Crystal Structures of Earth-Abundant Nontoxic Photovoltaic CuBil ₄ . Crystal Growth and Design, 2021, 21, 2850-2855. | 3.0 | 8 |
| 70 | Bandgap Engineering in the Configurational Space of Solid Solutions via Machine Learning: (Mg,Zn)O Case Study. Journal of Physical Chemistry Letters, 2021, 12, 5163-5168. | 4.6 | 8 |
| 71 | Breaking the Aristotype: Featurization of Polyhedral Distortions in Perovskite Crystals. Chemistry of Materials, 2022, 34, 562-573. | 6.7 | 8 |
| 72 | Stoichiometrically graded SiN <i>x</i> for improved surface passivation in high performance solar cells. Journal of Applied Physics, 2012, 112, . | 2.5 | 7 |

| # | Article | IF | CITATIONS |
|----|--|------|-----------|
| 73 | Lattice-mismatched heteroepitaxy of IV-VI thin films on PbTe(001): Anab initiostudy. Physical Review B, 2015, 91, . | 3.2 | 7 |
| 74 | Interpretable, calibrated neural networks for analysis and understanding of inelastic neutron scattering data. Journal of Physics Condensed Matter, 2021, 33, 194006. | 1.8 | 7 |
| 75 | A tunable amorphous p-type ternary oxide system: The highly mismatched alloy of copper tin oxide. Journal of Applied Physics, 2015, 118, 105702. | 2.5 | 5 |
| 76 | Machine Learning Approaches for Accelerating the Discovery of Thermoelectric Materials. ACS Symposium Series, 0, , 1-32. | 0.5 | 5 |
| 77 | Magnetic coupling in a hybrid Mn(<scp>ii</scp>) acetylene dicarboxylate. Physical Chemistry Chemical Physics, 2016, 18, 33329-33334. | 2.8 | 4 |
| 78 | MOFs modeling and theory: general discussion. Faraday Discussions, 2017, 201, 233-245. | 3.2 | 4 |
| 79 | Mixed-anion mixed-cation perovskite (FAPbl ₃) _{)(sub>)0.875} (MAPbBr ₃) _{0.125} : an <i>ab initio</i> molecular dynamics study. Journal of Materials Chemistry A, 2022, 10, 9592-9603. | 10.3 | 4 |
| 80 | Understanding the Balance of Entropy and Enthalpy in Hydrogen–Halide Noncovalent Bonding. Journal of Physical Chemistry Letters, 2020, 11, 3495-3500. | 4.6 | 3 |
| 81 | Revealing the crystal structures and relative dielectric constants of fluorinated silicon oxides. Journal of Materials Chemistry C, 2021, 9, 15983-15989. | 5.5 | 3 |
| 82 | Ultralow work function of the electride Sr ₃ CrN ₃ . Physical Chemistry Chemical Physics, 2022, 24, 8854-8858. | 2.8 | 3 |
| 83 | Quantum Statistical Transport Phenomena in Memristive Computing Architectures. Physical Review Applied, 2021, 15, . | 3.8 | 2 |
| 84 | UnlockNN: Uncertainty quantification for neural network models of chemical systems. Journal of Open Source Software, 2022, 7, 3700. | 4.6 | 2 |
| 85 | Ultrafast carrier dynamics in BiVO <inf>4</inf> : Interplay between free carriers, trapped carriers and low-frequency lattice vibrations. , 2016, , . | | 1 |
| 86 | Differentiating the role of organic additives to assemble open framework aluminosilicates using INS spectroscopy. Physical Chemistry Chemical Physics, 2020, 22, 14177-14186. | 2.8 | 1 |
| 87 | Computers in neutron science. Journal of Physics Communications, 2020, 4, 110401. | 1.2 | 1 |
| 88 | Local Coordination in Metal-Organic Frameworks Probed in the Vibrational and Optical Regime by EELS. Microscopy and Microanalysis, 2019, 25, 606-607. | 0.4 | 0 |